CHAP is a newly identified Z-disc protein essential for heart and skeletal muscle function

Abdelaziz Beqqali[1,2], Jantine Monshouwer-Kloots[1,2], Rui Monteiro[3], Maaike Welling[1], Jeroen Bakkers[1], Elisabeth Ehler[4], Arie Verkleij[5], Christine Mummery[1,2] and Robert Passier[1,2,*]

[1]Hubrecht Institute, Developmental Biology and Stem Cell Research, Uppsalalaan 8, 3584 CT, Utrecht, The Netherlands
[2]Leiden University Medical Center, Department of Anatomy and Embryology, Einthovenweg 20, 2333 ZC, Leiden, The Netherlands
[3]Molecular Hematology Unit, Weatherall Institute of Molecular Medicine (WIMM), University of Oxford, John Radcliffe Hospital, Headington, Oxford, OX3 9DS, UK
[4]The Randall Division of Cell & Molecular Biophysics and the Cardiovascular Division, King's College London, London SE1 1UL, UK
[5]Department of Cellular Architecture and Dynamics, Institute of Biomembranes, Utrecht University, Padualaan 8, 3584 CH, Utrecht, The Netherlands

*Author for correspondence (r.passier@lumc.nl)

Accepted 24 January 2010
Journal of Cell Science 123, 1141-1150

doi:10.1242/jcs.063859

Summary

In recent years, the perception of Z-disc function has changed from a passive anchor for myofilaments that allows transmission of force, to a dynamic multicomplex structure, capable of sensing and transducing extracellular signals. Here, we describe a new Z-disc protein, which we named CHAP (cytoskeletal heart-enriched actin-associated protein), expressed in differentiating heart and skeletal muscle in vitro and in vivo. Interestingly, in addition to its sarcomeric localization, CHAP was also able to translocate to the nucleus. CHAP was associated with filamentous actin in the cytoplasm and the nucleus when expressed ectopically in vitro, but in rat neonatal cardiomyocytes, CHAP disrupted the subcellular localization of α-actinin, another Z-disc protein. More importantly, knockdown of CHAP in zebrafish resulted in aberrant cardiac and skeletal muscle development and function. These findings suggest that CHAP is a critical component of the sarcomere with an important role in muscle development.

Key words: CHAP, Synpo2l, Z-disc, Heart development, Muscle, Sarcomere

Introduction

The sarcomere is bordered by the Z-discs and is the smallest contractile unit of striated muscle. Contractile sarcomeric proteins, such as actin and myosin, play essential roles in the assembly and maintenance of the sarcomere but cytoskeletal proteins are also crucial for structure integrity. The Z-disc, which is important for cross-linking of thin filaments and which functions as a nodal point in transmission of force generated within the sarcomere, has long been considered as the passive part of the contractile structure. A major component of the Z-disc is α-actinin-2, one of four highly similar (muscle and non-muscle) proteins that were originally described as actin crosslinking proteins. Besides its role in organizing the polarized orientation of actin, α-actinin may function as a platform for the assembly and interaction of multiprotein complexes. In striated muscle this is further supported by the findings that α-actinin-2 mediates molecular interconnections at the Z-disc by binding to different signalling molecules, such as the Rho effector PKN (Mukai et al., 1997), phospholipase D2 (Park et al., 2000) and G-protein coupled receptor kinases (Freeman et al., 2000), suggesting a role in several signalling pathways.

In recent years it has become clear that some Z-disc proteins, in particular those bound to or associated with actin and α-actinin, can respond to extracellular physical stimuli, such as stretch, stress or strain, by translocating to other cell compartments (Frank et al., 2006; Lange et al., 2006). One of the first Z-disc proteins implicated in mechano-signal transduction was the α-actinin-binding muscle LIM protein (MLP) (Arber et al., 1994; Knoll et al., 2002). In response to chronic pressure, MLP translocates from the cytoplasm to the nucleus (Ecarnot-Laubriet et al., 2000); here it can stimulate myogenic differentiation by binding to the muscle-specific transcription factor MyoD, which enhances transcriptional activity of downstream targets (Kong et al., 1997). Z-disc actin-binding proteins have also been shown to activate transcriptional responses. For example, striated muscle activator of Rho signalling (STARS) changes the ratio of the monomeric (G-actin) to polymerized (F-actin) form of actin by promoting polymerization (Arai et al., 2002). The resulting decrease in G-actin leads to activation of serum response factor (SRF), a transcription factor that regulates the muscle genetic program.

In addition to their involvement in transducing signalling events from different subcellular regions, actin- and α-actinin binding Z-disc proteins may also play roles in development or maintenance of both cardiac and skeletal muscle function. For example, *Cypher* (also known as ZASP/oracle) (Faulkner et al., 1999; Passier et al., 2000; Zhou et al., 1999) knockout mice display severe congenital myopathy and early postnatal death, demonstrating the necessity for Z-disc integrity in contracting muscle (Zhou et al., 2001). In zebrafish, knockdown of *cypher* leads to severe somite and heart defects during development (van der Meer et al., 2006). MLP-null mice by contrast, display normal heart and skeletal muscle development but dilated cardiomyopathy occurs postnatally (Arber et al., 1994).

We recently performed whole-genome microarray analysis on human embryonic stem cells (hESCs) differentiating towards cardiomyocytes, from which we identified multiple known and new cardiac-enriched genes (Beqqali et al., 2006). Among these we identified a novel heart-enriched gene, named Synaptopodin 2-like (*Synpo2l*). Here we show that this gene encodes a cytoskeletal

protein which is highly expressed in the Z-disc of heart and skeletal muscle, associates with actin and interacts with α-actinin. We thus renamed this protein cytoskeletal heart-enriched actin-associated protein (CHAP). CHAP was unexpectedly detected in the nucleus of embryonic cardiomyocytes and overexpression of CHAP in rat neonatal cardiomyocytes resulted in disorganization of α-actinin. These results were confirmed and further extended by knockdown of CHAP in zebrafish, which resulted in aberrant heart and skeletal muscle development, disorganized sarcomeres and ultimately lead to diminished cardiac contractility.

Results

Identification of CHAP

The mouse orthologue, which mapped to chromosome 14A3, was found after BLAST search with human CHAP (GenBank accession no. NM_024875). Amino acid sequence comparison revealed 85% identity between human and mouse CHAP (supplementary material Fig. S1A), and conservation amongst vertebrates (supplementary material Fig. S2). Cloning and sequencing of mouse CHAP showed that the predicted GenBank transcript (NM_175132.3) lacks nine coding base pairs (GTA TCT AAG, bp 97-105). The open reading frame (ORF) encodes a 978 amino acid (aa) protein. The predicted genomic organization of *Chap* revealed four exons of the *Chap* gene. Database searches identified expressed sequence tags (ESTs) that showed a non-predicted exon containing a start codon for a shorter isoform, which we termed CHAPb (supplementary material Fig. S1B-D). Cloning of *ChapB* revealed an ORF encoding a 749 aa protein.

Sequence comparisons showed that CHAPb has significant homology (31%) to myopodin (Synpo2) (Weins et al., 2001) and synaptopodin (30%) (Mundel et al., 1997), proteins involved in skeletal muscle and neuron differentiation, respectively. CHAPa contains a predicted N-terminal PDZ domain and a potential classic nuclear localization signal (NLS): KKRR (Hicks and Raikhel, 1995), whereas CHAPb only contains the NLS (supplementary material Fig. S1C). PDZ domains are found in diverse signalling proteins and can bind the carboxyl-terminal or internal peptide sequences of proteins thereby forming protein complexes involved in signalling or subcellular transport (Hung and Sheng, 2002).

CHAP is expressed in developing heart and skeletal muscle

Whole-mount in situ hybridization showed earliest *ChapB* expression in the mouse at embryonic day (E)7.75 in the cardiac crescent (Fig. 1A); this was maintained throughout cardiac development in both the atria and ventricles (Fig. 1B-E). From E9.5 or E10, *ChapB* was also expressed in somites, in particular the myotome, which gives rise to skeletal muscle (Fig. 1D,F). At E12.5, we could detect *ChapB* in embryonic limb muscles by in situ hybridization (data not shown). *ChapA*, by contrast, was not detected during development (up to E12.5 analysed by in situ hybridization). A developmental shift in the expression of the two forms of *Chap* was evident by semi-quantitative RT-PCR, *ChapA* being dominant in adult heart and skeletal muscle and *ChapB* in embryonic heart (Fig. 1G).

To study CHAP protein we generated an antibody recognizing both mouse CHAP isoforms. Western blot analysis of embryonic and adult mouse heart extracts revealed a 110 kDa band for CHAPb in embryonic heart and a 140 kDa band for CHAPa in adult heart and skeletal muscle. These bands co-migrated with ectopically expressed CHAPa and CHAPb, respectively (Fig. 1H). These data confirmed muscle-specific and stage-dependent expression of CHAPa and CHAPb isoforms.

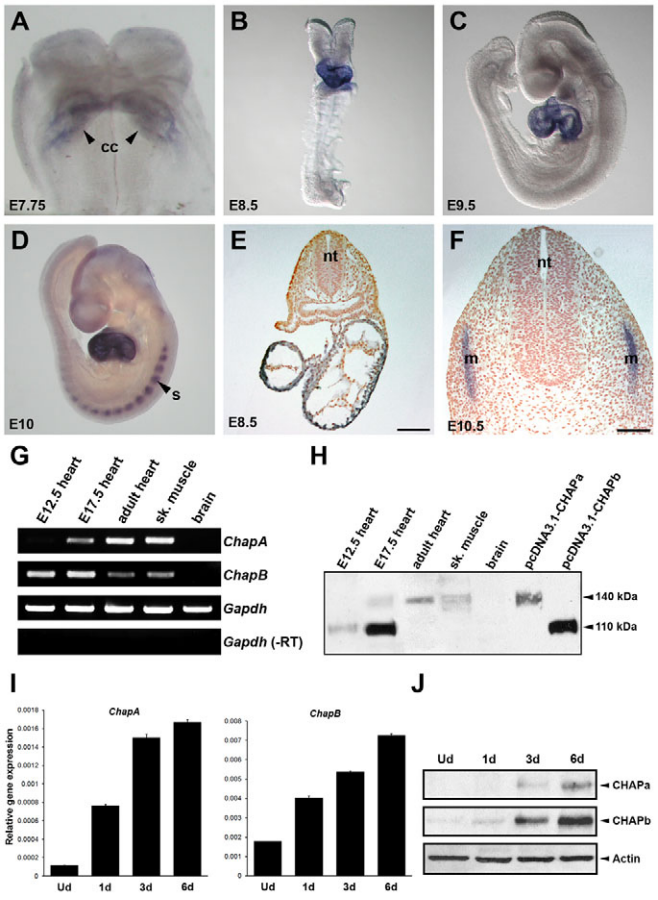

Fig. 1. Expression of CHAP in embryonic and adult mouse. (**A**) *ChapB* expression at E7.75 is restricted to the cardiac crescent. (**B**,**C**) *ChapB* is expressed ubiquitously in the heart at E8.5 and E9.5. (**D**) At E10 *ChapB* was also detected in the somites. (**E**) Transverse section of a E8.5 embryo shows *ChapB* expression throughout the heart. (**F**) Transverse section of E10.5 embryo shows expression of *ChapB* in the myotome. cc, cardiac crescent; s, somite; nt, neural tube; m, myotome. (**G**) Semi-quantitative RT-PCR shows that *ChapA* is absent in E12.5 heart but upregulated after E17.5 in heart and skeletal muscle. By contrast, *ChapB* is expressed in embryonic hearts (E12.5 and E17.5) and is downregulated in adult heart and skeletal muscle. Both *ChapA* and *B* are absent in adult brain. (**H**) Western blot analysis of endogenous CHAP in mouse tissues revealed a 140 kDa band for CHAPa in adult heart and skeletal muscle and a 110 kDa band for CHAPb in embryonic heart. Overexpressed CHAPa and -b in COS-1 cells served as positive control. (**I**,**J**) Quantitative RT-PCR and western blot of CHAPa and CHAPb during C2C12 myoblast differentiation. *Chap* mRNA levels are expressed relative to *Gapdh*, and actin was used as a loading control in western blotting. Ud, undifferentiated; d, days of differentiation.

We used C2C12 myoblasts to investigate CHAP expression during skeletal muscle differentiation. CHAPa and b transcripts and proteins were undetectable or at very low levels in undifferentiated myoblasts (Fig. 1I,J). CHAPa protein was only upregulated later in skeletal muscle differentiation at day 6, although at lower levels than CHAPb. CHAPb protein was upregulated at day 1 of differentiation and gradually increased until day 6 when differentiated myotubes formed (Fig. 1J).

CHAP colocalizes with α-actinin at the Z-disc of the sarcomere

Using the anti-CHAP antibody, the location of CHAP was determined in cultured E17.5 mouse cardiomyocytes (Fig. 2A), adult heart and skeletal muscle hindlimb cryosections (Fig. 2B,C). CHAP was present at the Z-disc in both heart and skeletal muscle, indicated by colocalization with α-actinin (Fig. 2A-C, upper panel), but not myomesin, an M-band marker (Fig. 2A-C, lower panel). Interestingly, CHAP was occasionally observed in the nucleus of cultured E17.5 cardiomyocytes (Fig. 2A, upper panel).

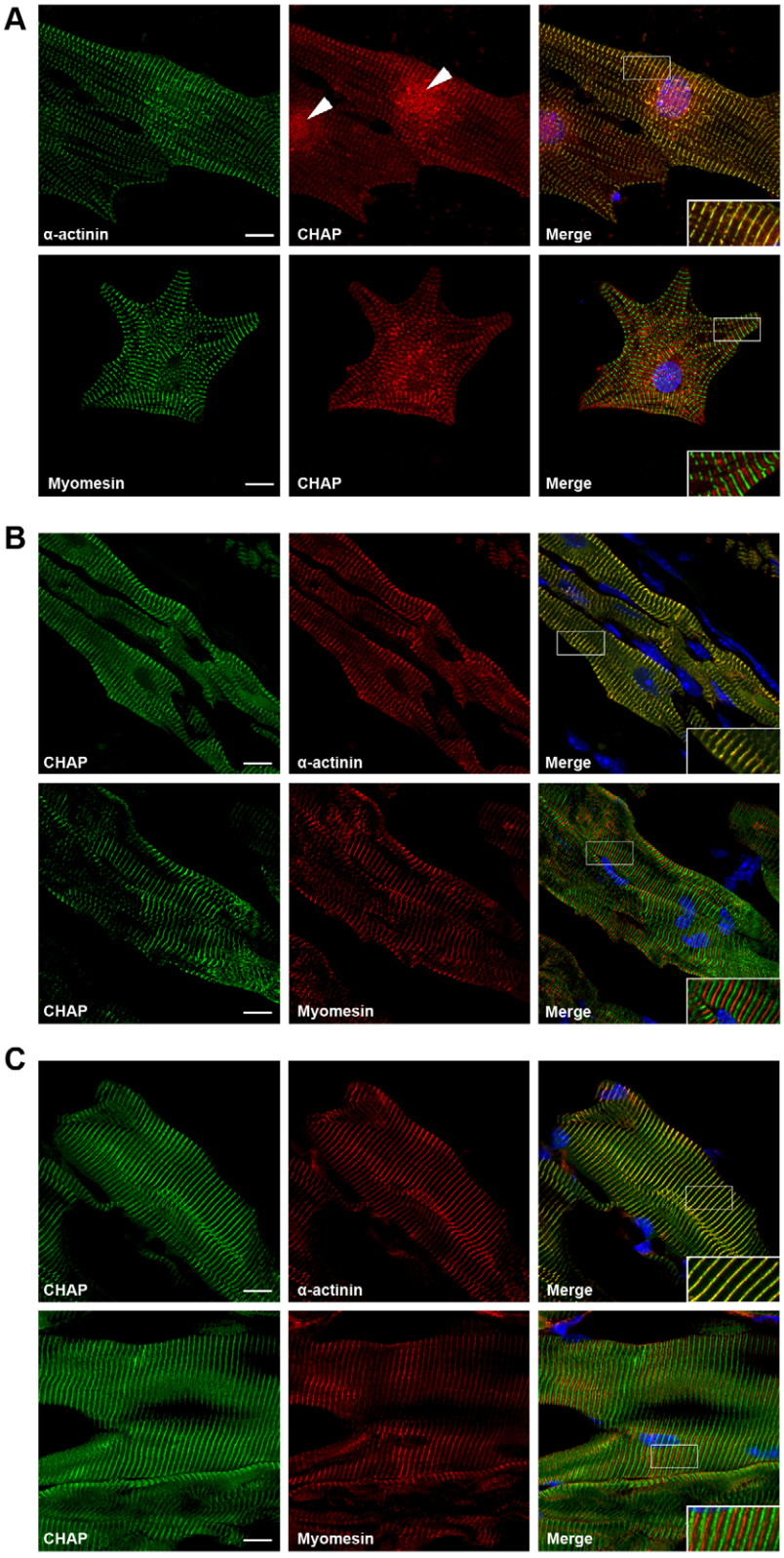

Ectopic expression of CHAP reveals actin association

Since highest homology of CHAP was observed with the actin-associated proteins, myopodin and synaptopodin, we expressed CHAP ectopically in COS-1 cells and determined whether it colocalized with actin. CHAPa-GFP showed a cytoskeletal organization, punctate cytoplasmic distribution and nuclear localization (supplementary material Fig. S4A). Colocalization of CHAPa-GFP with F-actin, as indicated by phalloidin staining, strongly suggested association with actin filaments. In addition, CHAPa formed nuclear actin-containing loops and rods, suggesting that CHAPa could bundle nuclear actin. Overexpression of CHAPb-GFP revealed similar results to that of CHAPa-GFP (supplementary material Fig. S4B).

Since CHAP colocalized with actin filaments, we investigated whether disruption of F-actin would affect CHAP localization. CHAPa/b-GFP-transfected COS-1 cells were cultured in the presence of cytochalasin D (CytoD), which disrupts actin filaments and inhibits actin polymerization (Goddette and Frieden, 1986). Both CHAPa- and CHAPb-GFP lost their cytoskeletal organization and showed punctate cytoplasmic and nuclear distribution, confirming CHAP association with actin (supplementary material Fig. S4C).

Domain mapping of CHAPa and b

We have performed domain mapping experiments by overexpressing truncated CHAP-GFP proteins in COS-1 cells (Fig. 3A). In contrast to the cytoskeletal and nuclear localization of full-length CHAPa in COS-1 cells (Fig. 3B) and sarcomeric localization in cardiomyocytes (Fig. 3C), the N-terminal 441aa of CHAPa containing the PDZ domain and the NLS, was found predominantly in the nucleus (Fig. 3B). However, nuclear localization was not dependent on

Fig. 2. *Chap* is localized at the Z-disc of the sarcomere. (**A**) Subcellular localization of CHAP in E17.5 mouse cardiomyocytes as shown by immunofluorescence. CHAP colocalizes with α-actinin at the Z-disc and is present in the nucleus (arrowheads, upper panel). CHAP does not colocalize with the M-band marker myomesin (lower panel). (**B**) Subcellular localization of CHAP in adult mouse heart cryosection. CHAP is not present in the nucleus of adult cardiomyocytes but is localized at the Z-disc, as shown by α-actinin colocalization (upper panel). CHAP is not colocalized with myomesin, an M-band marker (lower panel). (**C**) Subcellular localization of CHAP in adult skeletal muscle cryosections. CHAP is colocalized with α-actinin (upper panel) but not with myomesin (lower panel). Scale bar: 10 μm.

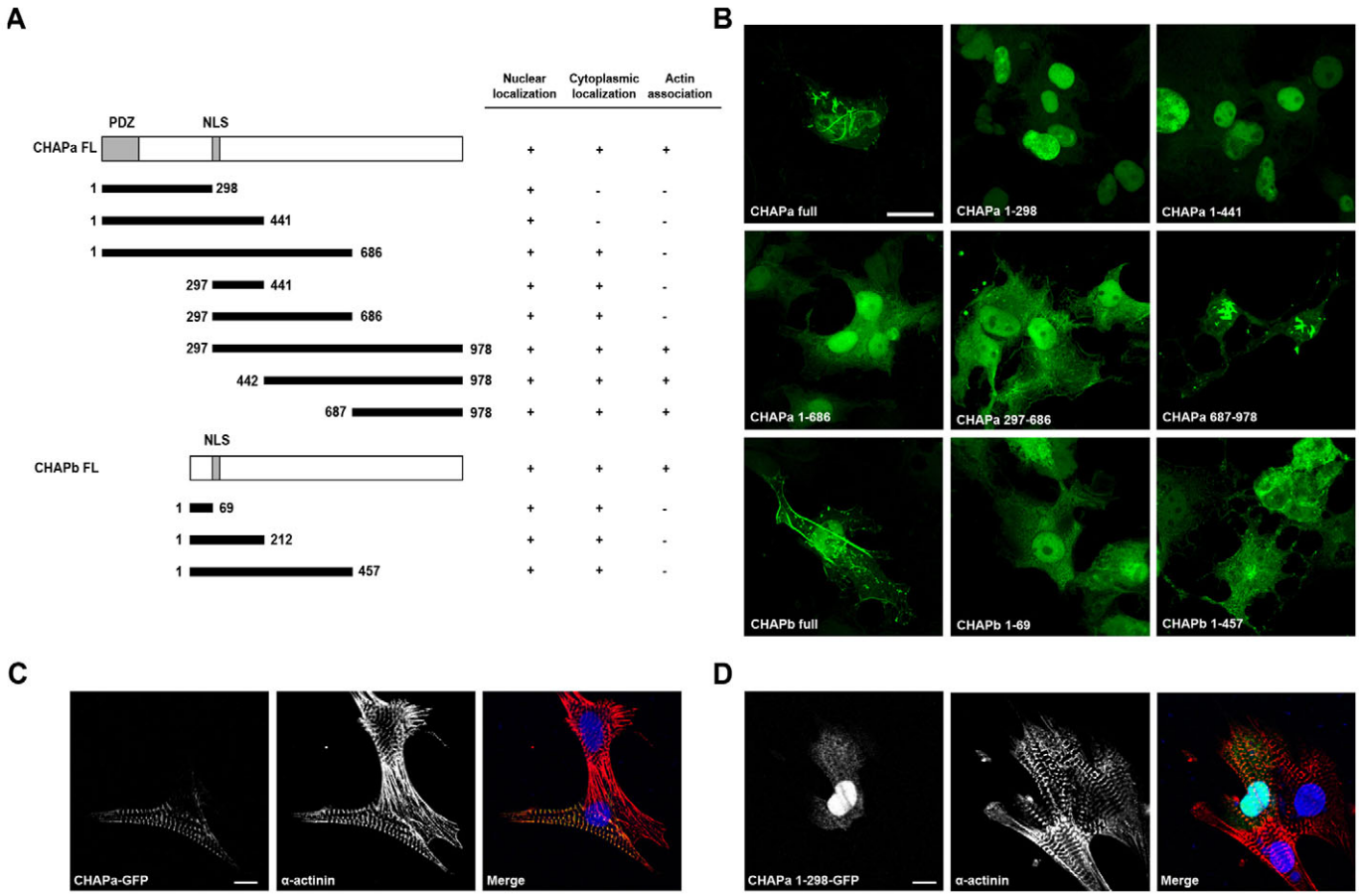

Fig. 3. Mapping of CHAP functional domains. (**A**) Schematic representation of truncated CHAP-GFP fusion proteins expressed in COS-1 cells and their individual subcellular localization and/or actin-association indicated by a + (presence) or – (absence). (**B**) Expression of CHAP-GFP truncations in COS-1 cells shows that the NLS is not necessary for nuclear localization, and the C-terminus of CHAP (CHAPa 687-978) is required for actin-association. Scale bar: 20 µm. (**C**) Immunostaining for α-actinin-2 in neonatal rat cardiomyocytes overexpressing CHAPa-GFP reveals localization of CHAPa-GFP at in the Z-disc of the sarcomere. (**D**) Expression of the N-terminal 298 aa of CHAPa in neonatal rat cardiomyocytes. Scale bars: 10 µm.

the NLS since aa 1-298 also displayed nuclear localization in both COS-1 cells and cardiomyocytes (Fig. 3B,D). In fact, CHAPa 297-441 (or CHAPb 68-212) contained the NLS but did not show exclusive nuclear localization. Diffuse cytoplasmic and nuclear localization was observed with CHAPa 1-686aa, suggesting that the characteristic cytoplasmatic and nuclear actin-association was determined by the C-terminal sequence. Indeed, CHAPa 687-978aa (or CHAPb 458-749aa) restored the actin-associated localization in both COS-1 cells (Fig. 3B) and cardiomyocytes (data not shown). Exclusive nuclear localization was never seen with any of the CHAPb fusion proteins.

In summary, the N-terminus containing the PDZ domain, but not the NLS, appears sufficient for nuclear localization. Furthermore, the cytoskeletal and nuclear actin association is regulated by the C-terminus, present in both CHAP isoforms.

CHAP interacts with α-actinin but not with actin

Since CHAP colocalized with α-actinin and actin, we investigated whether CHAP interacts with these proteins. We performed immunoprecipitation of actin using COS-1 cells expressing FLAG-CHAPb. However, no interaction was detected between CHAP and actin (Fig. 4A). Endogenous α-actinin was immunoprecipitated from C2C12 myotubes and analyzed for the presence of CHAP by western blotting (supplementary material Fig. S5, upper panel). CHAPb was co-immunoprecipitated with α-actinin whereas no α-actinin was detected in the negative control. Conversely, when endogenous CHAP was immunoprecipitated, α-actinin could be detected by western blot (supplementary material Fig. S5, lower panel). In addition, overexpression and immunoprecipitation of CHAPb and α-actinin in COS-1 cells confirmed their interaction (Fig. 4B).

Interestingly, when CHAPb-GFP was overexpressed in neonatal rat cardiomyocytes, α-actinin organization was disturbed and no longer restricted to the Z-disc, whereas myomesin localization in the M-band was unaffected. In non-transfected cells (GFP-negative adjacent cells) α-actinin was, as expected, localized in the Z-disc (Fig. 4C).

Identification and expression of the zebrafish *Chap* orthologue

To study the role of Chap in vivo we identified the *Chap* orthologue in zebrafish (*Danio rerio*) by searching the zebrafish Ensembl database using the mouse cDNA sequence for *ChapA*. Two putative genes were found, which we named *chap1* and *chap2* encoding proteins of 938 aa and 931 aa, respectively. Chap1 is more conserved compared to mouse (45%) or human CHAPa (45%) than Chap2 (43% and 43%, respectively), and there is 53% conservation

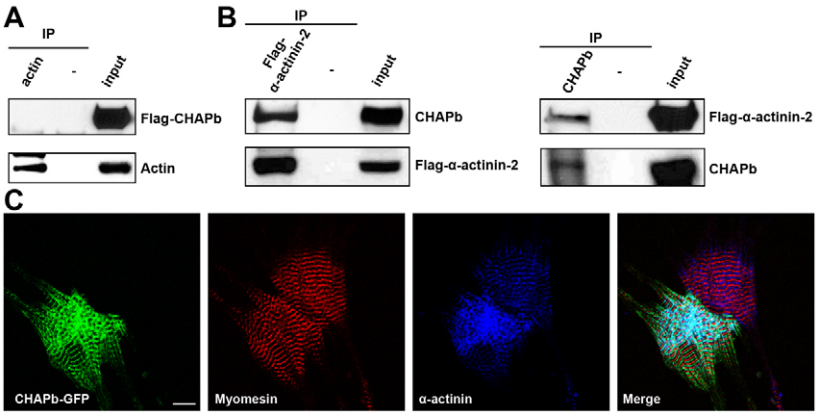

Fig. 4. CHAPb binds to α-actinin but not to actin. (**A**) Immunoprecipitation (IP) of actin from COS-1 cells expressing FLAG-CHAPb. No interaction with FLAG-CHAPb could be detected. (**B**) Co-IP of CHAPb with FLAG-α-actinin-2 using anti-FLAG for IP (left panel). Conversely, FLAG-α-actinin-2 co-IPed with CHAPb using CHAP antibody for IP (lower panel). (**C**) Immunostaining for α-actinin-2 in neonatal rat cardiomyocytes overexpressing CHAPb-GFP revealed disorganized α-actinin-2 while myomesin localization was unaffected. Untransfected adjacent cells showed normal α-actinin-2 expression. Scale bar: 10 μm.

between Chap1 and Chap2. However, important domains such as the PDZ, NLS and the C-terminal actin-association domain are highly conserved (supplementary material Fig. S6A).

Temporal and spatial expression of *chap1* and *chap2* mRNA were analyzed using semi-quantitative RT-PCR and whole-mount in situ hybridization in zebrafish embryos. RT-PCR showed that neither *chap1* nor *chap2* was expressed by 1-cell stage and 6 hours postfertilization (hpf) embryos but were detected from 24 hpf onwards until at least 6 dpf (Fig. 5A). *chap1* was detected by in situ hybridization in the somites and cardiac progenitors as early as the 3-somite stage. The somitic expression of *chap1* appeared confined to the adaxial cells. *chap1* was expressed in the cardiac progenitor cells at the 12-somite stage and later in the heart tube (Fig. 5B). At the 21-somite stage, *chap1* was expressed in the cardiac cone and in somites, in which expression was stronger at the somite boundaries. Expression at 24 hpf was in the somites and heart tube (Fig. 5B). *chap1* continued to be expressed in the heart, while somitic expression gradually decreased from 24 hpf until 48 hpf where it was absent in the somites. At 48 hpf, *chap1* is also expressed in the pectorial fin buds in addition to the heart (Fig. 5B). By contrast, *chap2* was expressed exclusively in the somites until 36 hpf when cardiac expression was observed for the first time (supplementary material Fig. S6Ba,Bb). Somitic and cardiac expression was maintained at low levels until at least 3 dpf (supplementary material Fig. S6Bc,Bd).

Chap is required for heart and skeletal muscle development

To determine the functions of Chap1 and Chap2 in vivo, we knocked down each gene product using antisense morpholino oligonucleotides (MOs) in zebrafish. Injection of *chap1* or *chap2* MOs caused defective somite development, aberrant heart morphology, decreased contractility and cardiac oedema (Fig. 6A). Furthermore, MO-injected embryos failed to hatch at 48 hpf; the chorion had to be removed manually, indicating reduced muscle force necessary for hatching (supplementary material Fig. S7B). Eventually, the Chap morphants deteriorated and embryos died at 6 dpf.

Since *chap1* was expressed earlier and at higher levels than *chap2*, we studied the *chap1* knockdown in zebrafish embryos in detail. At 3 dpf *chap1* morphants exhibited clear defects in heart and somite morphology and function. Morphant embryos were then divided into three groups depending on phenotype severity. 'Mild phenotype' embryos had kinked tails. 'Intermediate phenotype' embryos had bent tails and the pericardium was enlarged with defects in cardiac looping. 'Severely phenotype' morphants showed shortening of the body axis with tail coiling and the pericardium was enlarged with an elongated heart (supplementary material Fig. S7C).

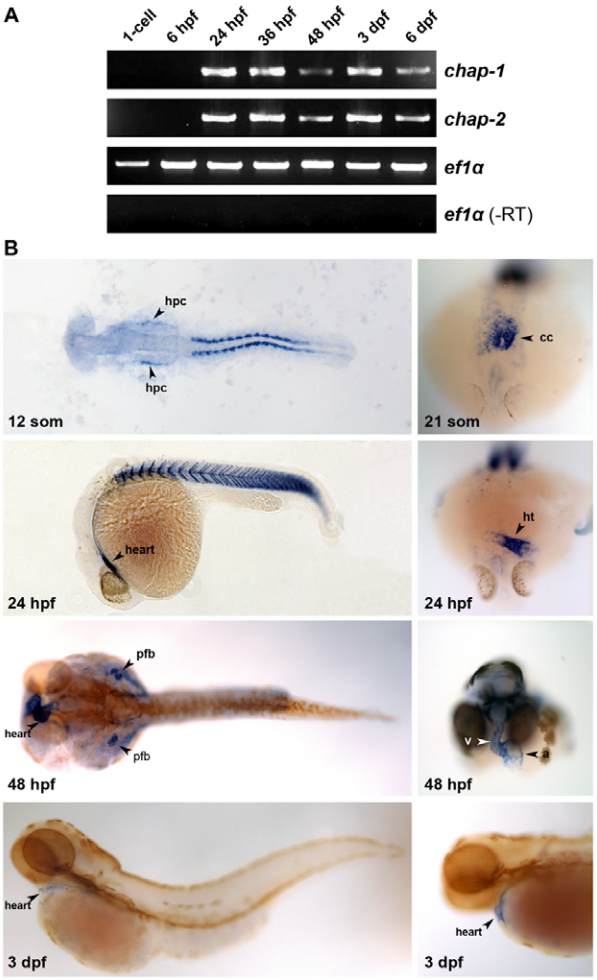

Fig. 5. Identification and expression of zebrafish *chap1* and *chap2*. (**A**) Semi-quantitative RT-PCR of zebrafish *chap1* and *chap2* during embryonic development. The *ef1α* housekeeping gene was used as control. *chap1* and *chap2* could not be detected at the 1-cell stage and 6 hpf, indicating that there was no maternal or zygotic expression of *chap*. (**B**) In situ hybridization of *chap1* during zebrafish development. hpc, heart progenitor cells; cc, cardiac cone; ht, heart tube; pfb, pectorial fin bud; v, ventricle; a, atrium.

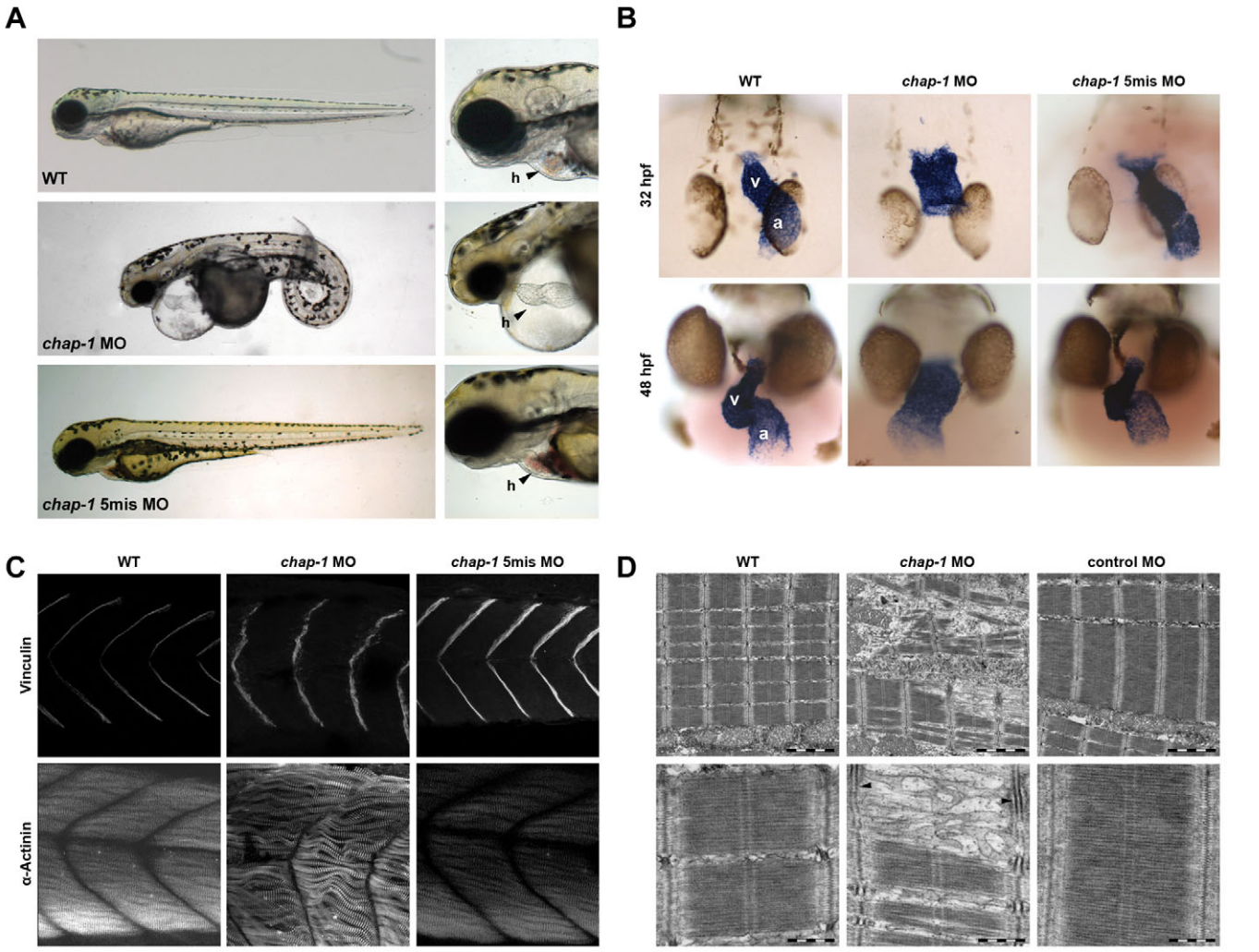

Fig. 6. Knockdown of *chap1* in zebrafish. (**A**) Morphological defects in *chap1* morpholino-mediated knockdown at 3 dpf. (Upper panel) Wild-type (WT) control embryo. (Middle panel) *chap1* morphant shows impaired trunk development and severe cardiac edema. (Lower panel) *chap1* 5-mismatch MO-injected embryo shows wild-type phenotype. h, heart. (**B**) In situ hybridization for the cardiac marker *cmlc2* in *chap1* morphants at 32 hpf and 48 hpf. *chap1* morphants show defective cardiac looping and broadening of the cardiac tube, whereas 5-mismatch MO-injected embryos have a correctly looped heart. a, atrium; v, ventricle. (**C**) Vinculin immunostaining of *chap1* morphants at 3 dpf (upper panel) reveals disturbed somite boundaries. Immunostaining for α-actinin of *chap1* morphants reveals disorganized myofibrils. (**D**) Ultrastructural analysis of somites of *chap1* morphants at 3 dpf. Wild-type and control MO-injected fish have normal sarcomere structure, whereas *chap1* morphants have severely disrupted Z-discs (arrowheads) and sarcomeres. Scale bars: 2 μm (upper panel); 500 nm (lower panel).

To assess cardiac morphogenesis and differentiation we examined *chap1* morphants for expression of the cardiac marker *cmlc2* by in situ hybridization. First defects became apparent at 32 hpf in the looping heart tube (Fig. 6B, upper panel). *chap1* morphants had a shortened, broad heart tube with a poorly defined atrio-ventricular boundary. Moreover, heart looping was strongly impaired, which became more obvious at 48 hpf (Fig. 6B, lower panel).

To investigate which part of the heart was most affected we performed in situ hybridization for the atrial marker aMHC and ventricular marker vMHC in *chap1* morphants (supplementary material Fig. S8). Broadening of both atrium and ventricle was observed at 32 hpf, whereas 5-mismatch MO-injected embryos had a correctly looped heart.

Somite boundaries, indicated by vinculin immunoreactivity were disrupted in *chap1* morphants, whereas the wild-type and 5-mismatch control morphants had normal chevron shaped somites (Fig. 6C, upper panel). Since integrin adhesion complexes are essential for force transmission (Dowling et al., 2008; Valencik et al., 2006) disruption of vinculin organization could explain the lack of muscle strength in *chap* morphants.

Since we showed that mouse CHAPb can bind to α-actinin-2 (Fig. 4B), we analyzed α-actinin-2 staining in *chap1* morphants. α-Actinin-2 was disorganized and muscle fibres were irregularly aligned in *chap1* morphants, whereas in *chap1* 5-mismatch controls α-actinin-2 organization and muscle fibre alignment was normal (Fig. 6C, lower panel).

At the ultrastructural level, sarcomeres in the skeletal muscle of *chap1* morphant embryos were absent or disorganized at 3 dpf. Furthermore, the Z-discs were disrupted where actin and myosin filaments were absent. This suggests a role for Chap in assembly of the Z-disc and anchoring of actin filaments. Sarcomere development was normal in control MO-injected fish (Fig. 6D).

Discussion

The Z-disc harbours many different proteins which take part in a network of interactions that are either involved in the transmission of force, the architecture of the sarcomere or as a mechano-sensor playing a role in signalling. Here, we report the identification of CHAP, a novel protein that interacts and colocalizes with α-actinin at the Z-disc of the sarcomere. Furthermore we showed that CHAP associates with polymerized actin, is able to translocate to the nucleus, and plays an important role in skeletal and cardiac muscle development. CHAP is specifically expressed in cardiac and skeletal muscle and is conserved amongst vertebrates, indicating an essential role in muscle function.

We identified two isoforms of mouse *Chap,* which we termed *ChapA* and *ChapB*. CHAPa contains an N-terminal PDZ domain and a classical NLS, which are both highly conserved amongst vertebrates. CHAPb lacks the N-terminal PDZ domain but contains the NLS. Examination of temporal and spatial expression showed that the short isoform *ChapB* was expressed at high levels during early heart and skeletal muscle development, whereas *ChapA* protein was only detected in adult muscle. A developmental shift of CHAP isoform expression was observed around E17.5, where we detected the first low level expression of *ChapA* mRNA and protein. CHAPa protein is expressed at higher level in adult heart and skeletal muscle, whereas CHAPb protein is undetectable. However, *ChapB* mRNA is still present at low levels in adult muscle. Furthermore, *ChapB* is expressed shortly after initiation of C2C12 myoblast differentiation, whereas *ChapA* is expressed at later stages of myogenic differentiation. However, CHAPb expression is higher in differentiated myotubes than CHAPa. This may be explained by taking in consideration that C2C12 myotubes may not represent fully mature adult skeletal muscle as present in vivo. Taken together, CHAPb can be regarded as the 'embryonic' isoform and CHAPa as the 'adult' isoform.

Highest homology of CHAP was found with myopodin (31%) and synaptopodin (30%), both of which are actin-bundling proteins that interact with α-actinin (Mundel et al., 1997; Weins et al., 2001). Synaptopodin is expressed in kidney and forebrain, whereas myopodin is expressed in skeletal muscle, but also at lower levels in heart and smooth muscle. Myopodin shuttles between the nucleus and the Z-disc, depending on the stage of differentiation and stress conditions (De Ganck et al., 2005; Weins et al., 2001). It has been demonstrated that nuclear import of myopodin is mediated by the binding of importin-α to two potential NLSs, regulated via binding to 14-3-3 (Faul et al., 2005). However, both NLSs of myopodin were not necessary for nuclear localization, suggesting the existence of an alternative nuclear import pathway. Indeed, importin 13, another nuclear transport protein has been shown to bind the C-terminus of myopodin (Liang et al., 2008). In agreement, we also showed that the CHAP NLS was not necessary for nuclear import since truncated fragments of CHAP, which lack the NLS, still localized to the nucleus even if the fragments exceeded 60 kDa, when nuclear entry by passive diffusion normally does not occur (Gorlich and Kutay, 1999). It is, therefore, likely that nuclear import of CHAP is at least partially mediated by another import mechanism.

Like myopodin and synaptopodin, CHAP was associated with cytoskeletal and nuclear actin filaments and exhibited actin-bundling activity. Treatment with cytochalasin D, an inhibitor of actin polymerization, resulted in the disruption of CHAP cytoskeletal organization. The actin-association domain of CHAP was located in the final 293 amino acids at the C-terminus of the CHAP protein, which does not contain a classical actin-binding site. In agreement, direct interaction between CHAP and actin could not be detected. Instead, we demonstrated an interaction of CHAP with the actin-binding protein, α-actinin, suggesting that CHAP is associated with actin via binding to α-actinin. This is further corroborated by the fact that synaptopodin has also been shown to bind and regulate actin-bundling via α-actinin-2 and -4 (Asanuma et al., 2005). Formation of nuclear actin-containing loops and rods following exogenous expression of CHAP were similar to that of myopodin (Weins et al., 2001) and supervillin (Wulfkuhle et al., 1999). The functional significance of these nuclear actin loops and rods remains to be elucidated. Various actin-bundling proteins have been shown to regulate gene transcription. For example supervillin was found to bind and enhance the transactivational activity of the androgen receptor (Ting et al., 2002).

The presence of a PDZ domain in the adult isoform, CHAPa, most probably adds extra functions to CHAP in mature muscle cells, since PDZ domain-containing proteins have been shown to play an important role in the transport, localization and assembly of large signalling complexes (Harris and Lim, 2001). Other N-terminal PDZ-domain-containing proteins have been described as localizing in the Z-disc and binding to α-actinin-2. An example is ALP, which is expressed in heart and skeletal muscle (Xia et al., 1997). Cypher (also known as Oracle and *ZASP*), is also localized in the Z-disc in heart and skeletal muscle, where it binds to the C-terminus of α-actinin via the PDZ domain of Cypher (Faulkner et al., 1999; Passier et al., 2000; Zhou et al., 1999). It seems unlikely that the PDZ domain of CHAP is necessary for the binding to α-actinin, since overexpression of full-length CHAPb, which lacks the PDZ domain, in cardiomyocytes showed localization to the Z-disc and interaction with α-actinin-2. Overexpression of the N-terminal region of CHAPa, containing the PDZ domain, led to nuclear localization in COS-1 cells (Fig. 3D). Furthermore, overexpression of full-length CHAPb in cardiomyocytes resulted in a disorganized pattern of α-actinin-2, which led us to study the role of CHAP in vivo.

The zebrafish is an excellent vertebrate model for studying heart development in vivo. Therefore, we first identified and characterized the orthologues of *chap* in zebrafish in order to understand its function in vivo. We found two orthologues which we named *chap1* and *chap2*.

In addition to sequence homology, conserved syntenic organization confirmed that these two genes are true *Chap* orthologues. Strikingly, in every vertebrate investigated, genes surrounding *Chap* are highly conserved. For instance, *myozenin-2* (encoding another Z-disc protein) is located immediately downstream of *Chap*, whereas *myozenin-1* is immediately downstream of *myopodin*. In the zebrafish genome, *myozenin-1* is located immediately downstream of zebrafish *myopodin* on both chromosomes 1 and 7.

chap1 is expressed in the earliest stages of cardiomyocyte specification in the cardiac progenitor cells and continues to be expressed in the heart. Furthermore, *chap1* was expressed at the earliest stages of somitogenesis, but was lost by 48 hpf. *chap2*, however, was not expressed in the heart until 36 hpf. Expression in the somites was apparent at the 12-somite stage and remained expressed until at least 3 dpf. In summary, both *chap1* and *chap2* are expressed in the heart and in the somites but in distinct temporal patterns. Knockdown of *chap1* and *chap2* individually by antisense morpholino oligonucleotides revealed an essential role in cardiac and skeletal muscle development and function, as shown by decreased cardiac contractility and looping defect, enlarged

pericardial sac, myofibrillar disarray, disruption of somite boundaries and sarcomeric integrity. Knockdown of the *chap* genes ultimately resulted in death at 6 dpf, ruling out any potential redundancy between Chap1 and Chap2. Another indication of muscle defect was identified by the failure of the Chap morphants to hatch, which is dependent on the combination of enzymatic secretion and contractile force.

It has been shown that Z-discs are important structures for the development of functional sarcomeres (Sanger et al., 1986; Wang et al., 2005). At the ultrastructural level we observed absence of sarcomeres and disrupted Z-discs in the somites of Chap1 morphants, indicating defective sarcomerogenesis, which explains the impaired cardiac and somite contractility. It has been shown recently that impairment of myofibrillogenesis by actin polymerization inhibitors cytochalasin B, D and latrunculin A, which also disrupt cytoskeletal organization of CHAP, prevent cardiac looping (Latacha et al., 2005; Manasek et al., 1978). MO-mediated knockdown of Cypher in zebrafish caused defective somite formation, enlargement of the pericardium and dilation of the ventricular wall, which resembled dilated cardiomyopathy (DCM) (van der Meer et al., 2006), underscoring the importance of Z-disc-associated PDZ-domain proteins in muscle development and function. In humans, mutations in Cypher have been associated with DCM and left ventricular non-compaction (Arimura et al., 2004; Vatta et al., 2003).

A few Z-disc proteins have been shown to localize in different compartments of the cell, such as the nucleus, and mutations in these proteins have been linked to cardiac and skeletal myopathies in humans and mice (Frank et al., 2006). Mice lacking the Z-disc protein MLP develop lethal cardiomyopathy (Arber et al., 1997). MLP has been implicated in mechanosignalling since there is evidence that MLP translocates between the cytoplasm and nucleus in response to physical stimuli such as (cardiac) chronic pressure overload (Ecarnot-Laubriet et al., 2000). Because of its unique position at the interface of the cytoskeleton and the sarcomere, the Z-disc has been suggested to play a role as a mechanosensor in cardiomyopathic chamber dilation (Knoll et al., 2002).

It would be of interest to further elucidate the molecular mechanisms and signalling events that are associated with the dual compartment protein CHAP in muscle development and disease. CHAP may play a dual role as a structural protein at the Z-disc and a regulator protein participating in a signalling pathway between the nucleus and the Z-disc in development and during cellular stress. Interestingly, we identified an embryonic as well as adult isoform of CHAP. Since re-expression of embryonic or foetal cardiac genes in adults is frequently observed in cardiac diseases, such as hypertrophy, it would be interesting to study CHAP isoforms in pathophysiological conditions.

Materials and Methods

Plasmid constructs

Full-length and truncated fragments of mouse CHAPa and CHAPb were amplified by PCR from mouse E17.5 heart cDNA and cloned into pCRII-TOPO or pcDNA6.2/C-EmGFP/TOPO expression vector (Invitrogen). cDNAs encoding mouse CHAPa and CHAPb with a N-terminal FLAG epitope were subcloned into pcDNA3.1 (Invitrogen). The pcDNA3.1/FLAG-α-actinin-2 expression construct was kindly provided by Norbert Frey, University of Kiel, Germany.

Zebrafish *chap1* and *chap2* were amplified by PCR from 36 hpf zebrafish cDNA and cloned into pCRII-TOPO (Invitrogen). All cloning products were confirmed by sequencing. Cloning primers are shown in supplementary material Table S1.

Production of polyclonal antibody

Polyclonal antiserum specific for CHAP was generated by immunization of rabbits (Eurogentec, Leuven, Belgium) with two synthetic peptides coding aa 827-841 [ARTLPNKAQSQGPRV] and aa 866-881 [CFDEGSSTPGPTSGPP] of mouse CHAPa (corresponding to aa 598-612 and aa 637-652 for CHAPb). For immunostaining and western blotting, IgG was purified from antiserum using protein-A-Sepharose beads (GE Healthcare). CHAP antibody specificity was verified by western blot analysis of different mouse tissue samples revealing two bands (140 kDa for CHAPa and 110 kDa for CHAPb), which were not present after preadsorption of the antibody with the peptides used for immunization (supplementary material Fig. S3A). CHAP antibody did not cross-react with myopodin (supplementary material Fig. S3B).

Cardiomyocyte isolation, cell culture and transient transfection

Rat neonatal cardiomyocytes, cultured from 1- to 3-day-old rats were prepared as described previously (Lange et al., 2002). Mouse E17.5 cardiomyocytes were isolated as described before (Maltsev et al., 1994). C2C12 myoblasts were cultured in Dulbecco's modified Eagle's medium (DMEM; Gibco-BRL) containing 10% foetal calf serum (FCS; Gibco-BRL). Differentiation was induced by replacing FCS with 2% horse serum (HS; Gibco-BRL) when cells reached 80% confluence. Differentiation medium was refreshed every day during differentiation until day 6. COS-1 cells were cultured in DMEM-F12 (Gibco-BRL) with 7.5% FCS. For immunocytochemistry, cells were plated on 0.1% gelatin-coated glass coverslips in a 12-well plate. COS-1 cells were transiently transfected using Lipofectamin 2000 (Invitrogen) and analyzed 48 hours after transfection. To disrupt F-actin fibres 10 μM cytochalasin D (Sigma) was added 48 hours post-transfection for 1 hour, before cells were fixed in 2% paraformaldehyde.

Immunocytochemistry

Cells on glass coverslips were fixed in 2% paraformaldehyde for 30 minutes, washed three times in PBS and permeabilized in 0.1% Triton-X100 in PBS for 8 minutes. Cells were blocked in 4% normal goat serum (NGS) for 1 hour at room temperature (RT) and then incubated with first antibody in 4% NGS for 1 hour at RT. Secondary antibody incubation occurred in 4% NGS for 1 hour at RT. Phalloidin-TRITC in PBS (1:500; Sigma-Aldrich) staining was performed after the secondary antibody step for 30 minutes at RT. Nuclear staining was performed as a last step using TO-PRO (Invitrogen) or DAPI (Molecular Probes). Coverslips were then mounted on glass slides using Mowiol (Calbiochem) and images were captured using confocal microscopy (Leica SPE). Primary antibodies were as follows: rabbit anti-CHAP (1:75; Eurogentec), mouse anti-α-actinin-2 (1:800; Sigma), mouse anti-myomesin (1:10; kindly provided by Elisabeth Ehler, King's College London, UK). Cy-3- and Cy-5-conjugated secondary antibodies were used at 1:250 (Jackson Immunoresearch Laboratories). Alexa-Fluor-488-conjugated secondary antibody was used at 1:100 (Invitrogen).

Immunohistochemistry

Heart and skeletal muscle cryosections were stained as described before (van Laake et al., 2006). Primary antibodies were used as follows: rabbit anti-CHAP (1:50; Eurogentec), mouse anti-α-actinin-2 (1:800; Sigma), mouse anti-myomesin (1:10; E. Ehler). Cy-3- and Cy-5-conjugated secondary antibodies were used at 1:250 (Jackson Immunoresearch Laboratories).

For zebrafish, immunofluorescence staining protocols were as previously described (Dong et al., 2007). The following antibodies were used: vinculin (1:200; Sigma) α-actinin (sarcomeric; 1:400; Sigma). Alexa-Fluor-488- (1:100; Invitrogen) and Cy-3- (1:250; Jackson Immunoresearch Laboratories) conjugated secondary antibody were used.

RT-PCR

Total RNA was isolated from cells using TRIzol reagent (Invitrogen) according to a standard protocol. DNAseI digestion was performed to ensure elimination of genomic DNA. Total RNA (1 μg) was transcribed by reverse transcriptase (SuperScript™ II RT, Invitrogen) and used for PCR using Silverstar DNA polymerase (Eurogentec) or Platinum Taq DNA polymerase HiFi (Invitrogen). For each PCR reaction, 1 μl cDNA was used in a reaction volume of 50 μl. The cycling parameters were 94°C for 15 seconds; 58°C, 30 seconds; and 72°C, 45 seconds, for 35 cycles. The PCR cycles were preceded by an initial denaturation for 2 minutes at 94°C and followed by a final extension for 7 minutes at 72°C. Glyceraldehyde phosphate dehydrogenase (*Gapdh*) was used as RNA input control. As a negative control, total RNA was used directly for PCR. Primers were, *ChapA* (sense: 5′-GAGGAGGTGCAGGTCACATT-3′; antisense: 5′-CTGAAGAGCCTGGGAAACAG-3′), *ChapB* (sense: 5′-GGC-TTTAAAGGGCCTTGG-3′; antisense: 5′-CCGCCGCTTCTTAAACATAA-3′), *Gapdh* (sense: 5′-GTTTGTGATGGGTGTGAACCAC-3′; antisense: 5′-CTGG-TCCTCAGTGTAGCCCAA-3′) zebrafish *ef1α* (sense: 5′-GGCCACGTCGACT-CCGGAAAGTCC-3′; antisense: 5′-CTCAAAACGAGCCTGGCTGTAAGG-3′), zebrafish *chap1* (sense: 5′-TCACTGTATATCCCTGCCAGACCA-3′; antisense: 5′-GCTCTCGAGAAGAGATCCCATCAG-3′) and zebrafish *chap2* (sense: 5′-CCA-CCACCAACTCCTCTACC-3′; antisense: 5′-GCCTGAGGGATCTGTGACATT-TCT-3′).

Real-time qPCR

Real-time PCR was performed according to standard protocols on a MyIQ single colour real-time PCR detection system (Bio-Rad). Briefly, 1 μg of total RNA was

treated with DNAse, and transcribed to cDNA. 10 µl of a 1/10 dilution of cDNA was then added to 12.5 µl of the 2× SYBR green PCR mastermix (Applied Biosystems, Foster City, CA, USA), and 500 µM of each primer. PCR cycles were 3 minutes at 95°C, followed by 40 cycles of 15 seconds at 95°C, 30 seconds at a specific annealing temperature, and 45 seconds at 72°C. The thermal denaturation protocol was run at the end of the PCR to determine the number of products. Samples were run on a 2% agarose gel to confirm the correct size of the PCR products. All reactions were run in triplicate. As negative controls, PCR was performed on water and on RNA without reverse transcription. The cycle number at which the reaction crossed an arbitrarily placed threshold (Cτ) was determined for each gene. The relative amount of mRNA levels was determined by $2^{-\Delta C\tau}$. Relative gene expression was normalized to *Gapdh* expression. Primer sequences and annealing temperatures used for real-time PCR are the same as described for RT-PCR above.

Immunoprecipitation and western blotting

For immunoprecipitation, cells were lysed in ice-cold RIPA-buffer (50 mM Tris-HCl, 150 mM NaCl, 1% NP-40, 0.2% sodium deoxycholate, 0.1% SDS) supplemented with dithiothreitol (DTT), phenylmethylsulphonyl fluoride (PMSF) and protease inhibitor cocktail (Sigma). Cell debris was spun down by centrifuging at 10,000 ***g*** for 15 min. Cell lysates were incubated overnight at 4°C with 1 µg/ml of antibody for immunoprecipitation. Antibodies used were as follows: anti-actin antibody C4 (Chemicon), anti-FLAG M2 (Sigma), anti-α-actinin2 (Sigma), and anti-CHAP. Subsequently, 30 µl protA/G beads (Santa Cruz Biotechnology) per ml lysate were added and incubated for 1 hour rotating at 4°C. Prot A/G beads were washed four times with RIPA buffer, resuspended in Laemmli sample buffer and boiled. Negative controls were performed by using an isotype control antibody for immunoprecipitation.

Western blotting was performed according to standard protocols. Briefly, protein concentrations were determined using the Bio-Rad protein assay and proteins were resolved by SDS-PAGE and transferred to polyvindyline difluoride (PVDF) membrane (GE Healthcare/Amersham). Primary antibodies were as follows: rabbit polyclonal anti-CHAP (1:200), mouse monoclonal anti-actin C4 (1:500; Chemicon), mouse monoclonal anti-FLAG M2 (1:1000; Sigma), mouse monoclonal anti-sarcomeric α-actinin2 (1:1000; Sigma). Horseradish peroxidase-conjugated secondary antibodies were used for detection. Western blots were developed with enhanced chemiluminescence (Pierce SuperSignal West Pico ECL) and exposed to film.

Microscopic imaging

To permit imaging, zebrafish embryos were dechorionated with forceps and anesthetized with MS-222. Embryos were analyzed under a Leica MZ FL III microscope and pictures were taken with a Leica DC 300F digital camera (Leica Microsystems). In situ hybridizations were imaged using a Zeiss Axioplan coupled to a Leica DFC480 digital camera. Immunofluorescence in cells and zebrafish embryos was imaged with a Leica TCS SPE confocal microscope (Leica Microsystems).

For electron microscopy, zebrafish embryos of 3 dpf were fixed in half-strength Karnovsky fixative as described in Karnovsky et al. (Karnovsky, 1965). Sections of 60 nm were cut using a Leica ultra-cryomicrotome and Diatome diamond knife and examined with a JEOL 1010 electron microscope at 80 kV.

Whole-mount in situ hybridization

Whole-mount in situ hybridization for mouse embryos was performed as described before (Beqqali et al., 2006). Probe template primers were designed with the T3-promoter sequence (5′-ATACAATTAACCCTCACTAAAGGG-3′) at the 5′ end of the forward primer and T7-promoter sequence (5′-ATAGGTAATACGACTC-ACTATAGGGC-3′) at the 5′ end of the reverse primer. Digoxigenin-labelled probes were generated using the purified PCR product as a template for probe transcription with either T3 RNA polymerase or T7 RNA polymerase (Promega, Madison, USA). Probe template primers are shown in supplementary material Table S2. For zebrafish embryos, whole-mount in situ hybridization was performed using digoxigenin-labelled antisense RNA probes, as described previously (Thisse et al., 1993). A combination of 4-nitro blue tetrazolium (NBT) and 5-bromo-4-chloro-3-indolyl phosphate 4-toluidine salt (BCIP) was used for detection. Sense RNA probes were used as negative control for each specific gene of interest. Embryos were cleared in methanol and mounted in benzylbenzoate and benzylalcohol (2:1) for photography.

Fish maintenance

Techniques for the care and breeding of zebrafish were according to standard protocols. Embryos were obtained from natural matings after the initiation of the light cycle, and staged as hours postfertilization (hpf) according to morphological criteria (Kimmel et al., 1995).

Morpholino antisense oligonucleotide injections

Stock morpholino oligonucleotides (Genetools, Philomath, OR) were dissolved in 1× Danieu's buffer (58 mM NaCl, 0.7 mM KCl, 0.4 mM $MgSO_4$, 5 mM HEPES, pH 7.6) (Nasevicius and Ekker, 2000). The diluted MO stocks (1 nl) were injected into one-cell stage zebrafish embryos. Non-specific MOs and gene-specific 5-mismatch MOs were used as controls. Specific MO-mediated knockdown was verified by GFP intensity following injection of *chap1-GFP* and *chap2-GFP,* both containing MO targeting sequences upstream of GFP, with or without co-injection of MOs (supplementary material Fig. S7A). The effective concentration for each morpholino was determined through dose-response experiments. Injection of 0.1 mM (0.8 ng) *chap1* MO or 0.2 mM (1.7 ng) *chap2* MO per embryo caused specific muscular defects with no observable defects in other structures, along with no significant increase in mortality in the randomized control MO or 5-mismatch-MO-injected embryos when injecting same amounts of MO.

MO sequences were as follows: control MO, 5′-CCTCTTACCTCAGTTA-CAATTTATA-3′; *chap1* MO^{ATG}, 5′-ACCACCTCCTCTGCTACCATTTTCC-3′; *chap1* 5mis MO^{ATG}5′-ACGACCTGCTGTGCTACGATTTTGC-3′; *chap2* MO^{ATG}, 5′-GATGATAACCTCCTCGGCCACCATG-3′; *chap2* 5mis MO^{ATG}, 5′-GATCA-TAAGCTGCTCCGCCAGCATG-3′.

We thank J. Verwey, L. du Puy and E. G. van Donselaar for technical assistance and J. Korving for histology. This study was supported by Bsik Programme 'Stem Cells in Development and Disease' (A.B.), the Netherlands Heart Foundation grant 2006B209 (R.P.), Portuguese Fundação para a Ciência e Tecnologia (R.M.) and by European Community's Sixth Framework Programme contract ('HeartRepair') LSHM-CT-2005-018630 (A.B. and R.P.).

Supplementary material available online at
http://jcs.biologists.org/cgi/content/full/123/7/1141/DC1

References

Arai, A., Spencer, J. A. and Olson, E. N. (2002). STARS, a striated muscle activator of Rho signaling and serum response factor-dependent transcription. *J. Biol. Chem.* **277**, 24453-24459.

Arber, S., Halder, G. and Caroni, P. (1994). Muscle LIM protein, a novel essential regulator of myogenesis, promotes myogenic differentiation. *Cell* **79**, 221-231.

Arber, S., Hunter, J. J., Ross, J., Jr, Hongo, M., Sansig, G., Borg, J., Perriard, J. C., Chien, K. R. and Caroni, P. (1997). MLP-deficient mice exhibit a disruption of cardiac cytoarchitectural organization, dilated cardiomyopathy, and heart failure. *Cell* **88**, 393-403.

Arimura, T., Hayashi, T., Terada, H., Lee, S. Y., Zhou, Q., Takahashi, M., Ueda, K., Nouchi, T., Hohda, S., Shibutani, M. et al. (2004). A Cypher/ZASP mutation associated with dilated cardiomyopathy alters the binding affinity to protein kinase C. *J. Biol. Chem.* **279**, 6746-6752.

Asanuma, K., Kim, K., Oh, J., Giardino, L., Chabanis, S., Faul, C., Reiser, J. and Mundel, P. (2005). Synaptopodin regulates the actin-bundling activity of alpha-actinin in an isoform-specific manner. *J. Clin. Invest.* **115**, 1188-1198.

Beqqali, A., Kloots, J., Ward-van Oostwaard, D., Mummery, C. and Passier, R. (2006). Genome-wide transcriptional profiling of human embryonic stem cells differentiating to cardiomyocytes. *Stem Cells* **24**, 1956-1967.

De Ganck, A., Hubert, T., Van Impe, K., Geelen, D., Vandekerckhove, J., De Corte, V. and Gettemans, J. (2005). A monopartite nuclear localization sequence regulates nuclear targeting of the actin binding protein myopodin. *FEBS Lett.* **579**, 6673-6680.

Dong, P. D., Munson, C. A., Norton, W., Crosnier, C., Pan, X., Gong, Z., Neumann, C. J. and Stainier, D. Y. (2007). Fgf10 regulates hepatopancreatic ductal system patterning and differentiation. *Nat. Genet.* **39**, 397-402.

Dowling, J. J., Gibbs, E., Russell, M., Goldman, D., Minarcik, J., Golden, J. A. and Feldman, E. L. (2008). Kindlin-2 is an essential component of intercalated discs and is required for vertebrate cardiac structure and function. *Circ. Res.* **102**, 423-431.

Ecarnot-Laubriet, A., De Luca, K., Vandroux, D., Moisant, M., Bernard, C., Assem, M., Rochette, L. and Teyssier, J. R. (2000). Downregulation and nuclear relocation of MLP during the progression of right ventricular hypertrophy induced by chronic pressure overload. *J. Mol. Cell Cardiol.* **32**, 2385-2395.

Faul, C., Huttelmaier, S., Oh, J., Hachet, V., Singer, R. H. and Mundel, P. (2005). Promotion of importin alpha-mediated nuclear import by the phosphorylation-dependent binding of cargo protein to 14-3-3. *J. Cell Biol.* **169**, 415-424.

Faulkner, G., Pallavicini, A., Formentin, E., Comelli, A., Ievolella, C., Trevisan, S., Bortoletto, G., Scannapieco, P., Salamon, M., Mouly, V. et al. (1999). ZASP: a new Z-band alternatively spliced PDZ-motif protein. *J. Cell Biol.* **146**, 465-475.

Frank, D., Kuhn, C., Katus, H. A. and Frey, N. (2006). The sarcomeric Z-disc: a nodal point in signalling and disease. *J. Mol. Med.* **84**, 446-468.

Freeman, J. L., Pitcher, J. A., Li, X., Bennett, V. and Lefkowitz, R. J. (2000). alpha-Actinin is a potent regulator of G protein-coupled receptor kinase activity and substrate specificity in vitro. *FEBS Lett.* **473**, 280-284.

Goddette, D. W. and Frieden, C. (1986). Actin polymerization. The mechanism of action of cytochalasin D. *J. Biol. Chem.* **261**, 15974-15980.

Gorlich, D. and Kutay, U. (1999). Transport between the cell nucleus and the cytoplasm. *Annu. Rev. Cell Dev. Biol.* **15**, 607-660.

Harris, B. Z. and Lim, W. A. (2001). Mechanism and role of PDZ domains in signaling complex assembly. *J. Cell Sci.* **114**, 3219-3231.

Hicks, G. R. and Raikhel, N. V. (1995). Nuclear localization signal binding proteins in higher plant nuclei. *Proc. Natl. Acad. Sci. USA* **92**, 734-738.

Hung, A. Y. and Sheng, M. (2002). PDZ domains: structural modules for protein complex assembly. *J. Biol. Chem.* **277**, 5699-5702.

Karnovsky, M. J. (1965). A formaldehyde-glutaraldehyde fixative of light osmolality for use in electron microscopy. *J. Cell Biol.* **27**, 137A-138A.

Kimmel, C. B., Ballard, W. W., Kimmel, S. R., Ullmann, B. and Schilling, T. F. (1995). Stages of embryonic development of the zebrafish. *Dev. Dyn.* **203**, 253-310.

Knoll, R., Hoshijima, M., Hoffman, H. M., Person, V., Lorenzen-Schmidt, I., Bang, M. L., Hayashi, T., Shiga, N., Yasukawa, H., Schaper, W. et al. (2002). The cardiac mechanical stretch sensor machinery involves a Z disc complex that is defective in a subset of human dilated cardiomyopathy. *Cell* **111**, 943-955.

Kong, Y., Flick, M. J., Kudla, A. J. and Konieczny, S. F. (1997). Muscle LIM protein promotes myogenesis by enhancing the activity of MyoD. *Mol. Cell. Biol.* **17**, 4750-4760.

Lange, S., Auerbach, D., McLoughlin, P., Perriard, E., Schafer, B. W., Perriard, J. C. and Ehler, E. (2002). Subcellular targeting of metabolic enzymes to titin in heart muscle may be mediated by DRAL/FHL-2. *J. Cell Sci.* **115**, 4925-4936.

Lange, S., Ehler, E. and Gautel, M. (2006). From A to Z and back? Multicompartment proteins in the sarcomere. *Trends Cell Biol.* **16**, 11-18.

Latacha, K. S., Remond, M. C., Ramasubramanian, A., Chen, A. Y., Elson, E. L. and Taber, L. A. (2005). Role of actin polymerization in bending of the early heart tube. *Dev. Dyn.* **233**, 1272-1286.

Liang, J., Ke, G., You, W., Peng, Z., Lan, J., Kalesse, M., Tartakoff, A. M., Kaplan, F. and Tao, T. (2008). Interaction between importin 13 and myopodin suggests a nuclear import pathway for myopodin. *Mol. Cell. Biochem.* **307**, 93-100.

Maltsev, V. A., Wobus, A. M., Rohwedel, J., Bader, M. and Hescheler, J. (1994). Cardiomyocytes differentiated in vitro from embryonic stem cells developmentally express cardiac-specific genes and ionic currents. *Circ. Res.* **75**, 233-244.

Manasek, F. J., Kulikowski, R. R. and Fitzpatrick, L. (1978). Cytodifferentiation: a causal antecedent of looping? *Birth Defects Orig. Artic. Ser.* **14**, 161-178.

Mukai, H., Toshimori, M., Shibata, H., Takanaga, H., Kitagawa, M., Miyahara, M., Shimakawa, M. and Ono, Y. (1997). Interaction of PKN with alpha-actinin. *J. Biol. Chem.* **272**, 4740-4746.

Mundel, P., Heid, H. W., Mundel, T. M., Kruger, M., Reiser, J. and Kriz, W. (1997). Synaptopodin: an actin-associated protein in telencephalic dendrites and renal podocytes. *J. Cell Biol.* **139**, 193-204.

Nasevicius, A. and Ekker, S. C. (2000). Effective targeted gene 'knockdown' in zebrafish. *Nat. Genet.* **26**, 216-220.

Park, J. B., Kim, J. H., Kim, Y., Ha, S. H., Yoo, J. S., Du, G., Frohman, M. A., Suh, P. G. and Ryu, S. H. (2000). Cardiac phospholipase D2 localizes to sarcolemmal membranes and is inhibited by alpha-actinin in an ADP-ribosylation factor-reversible manner. *J. Biol. Chem.* **275**, 21295-21301.

Passier, R., Richardson, J. A. and Olson, E. N. (2000). Oracle, a novel PDZ-LIM domain protein expressed in heart and skeletal muscle. *Mech. Dev.* **92**, 277-284.

Sanger, J. M., Mittal, B., Pochapin, M. B. and Sanger, J. W. (1986). Myofibrillogenesis in living cells microinjected with fluorescently labeled alpha-actinin. *J. Cell Biol.* **102**, 2053-2066.

Thisse, C., Thisse, B., Schilling, T. F. and Postlethwait, J. H. (1993). Structure of the zebrafish snail1 gene and its expression in wild-type, spadetail and no tail mutant embryos. *Development* **119**, 1203-1215.

Ting, H. J., Yeh, S., Nishimura, K. and Chang, C. (2002). Supervillin associates with androgen receptor and modulates its transcriptional activity. *Proc. Natl. Acad. Sci. USA* **99**, 661-666.

Valencik, M. L., Zhang, D., Punske, B., Hu, P., McDonald, J. A. and Litwin, S. E. (2006). Integrin activation in the heart: a link between electrical and contractile dysfunction? *Circ. Res.* **99**, 1403-1410.

van der Meer, D. L., Marques, I. J., Leito, J. T., Besser, J., Bakkers, J., Schoonheere, E. and Bagowski, C. P. (2006). Zebrafish cypher is important for somite formation and heart development. *Dev. Biol.* **299**, 356-372.

van Laake, L. W., van den Driesche, S., Post, S., Feijen, A., Jansen, M. A., Driessens, M. H., Mager, J. J., Snijder, R. J., Westermann, C. J., Doevendans, P. A. et al. (2006). Endoglin has a crucial role in blood cell-mediated vascular repair. *Circulation* **114**, 2288-2297.

Vatta, M., Mohapatra, B., Jimenez, S., Sanchez, X., Faulkner, G., Perles, Z., Sinagra, G., Lin, J. H., Vu, T. M., Zhou, Q. et al. (2003). Mutations in Cypher/ZASP in patients with dilated cardiomyopathy and left ventricular non-compaction. *J. Am. Coll. Cardiol.* **42**, 2014-2027.

Wang, J., Shaner, N., Mittal, B., Zhou, Q., Chen, J., Sanger, J. M. and Sanger, J. W. (2005). Dynamics of Z-band based proteins in developing skeletal muscle cells. *Cell Motil. Cytoskeleton* **61**, 34-48.

Weins, A., Schwarz, K., Faul, C., Barisoni, L., Linke, W. A. and Mundel, P. (2001). Differentiation- and stress-dependent nuclear cytoplasmic redistribution of myopodin, a novel actin-bundling protein. *J. Cell Biol.* **155**, 393-404.

Wulfkuhle, J. D., Donina, I. E., Stark, N. H., Pope, R. K., Pestonjamasp, K. N., Niswonger, M. L. and Luna, E. J. (1999). Domain analysis of supervillin, an F-actin bundling plasma membrane protein with functional nuclear localization signals. *J. Cell Sci.* **112**, 2125-2136.

Xia, H., Winokur, S. T., Kuo, W. L., Altherr, M. R. and Bredt, D. S. (1997). Actinin-associated LIM protein: identification of a domain interaction between PDZ and spectrin-like repeat motifs. *J. Cell Biol.* **139**, 507-515.

Zhou, Q., Ruiz-Lozano, P., Martone, M. E. and Chen, J. (1999). Cypher, a striated muscle-restricted PDZ and LIM domain-containing protein, binds to alpha-actinin-2 and protein kinase C. *J. Biol. Chem.* **274**, 19807-19813.

Zhou, Q., Chu, P. H., Huang, C., Cheng, C. F., Martone, M. E., Knoll, G., Shelton, G. D., Evans, S. and Chen, J. (2001). Ablation of Cypher, a PDZ-LIM domain Z-line protein, causes a severe form of congenital myopathy. *J. Cell Biol.* **155**, 605-612.

Table S1 Cloning primers

Construct	Forward primer	Reverse primer
mCHAPa	5'-CACCATGGGTGCTGAGGAGGAGGTG-3'	5'-CTGGTGCCCTGCCCCAGGCCT-3'
mCHAPb	5'-CACCATGGAGACCACCATCCAAGAGCCCCTC-3'	5'-CTGGTGCCCTGCCCCAGGCCT-3'
FLAG-mCHAPa	5'-CACCATGGACTACAAGGATGACGACGACAAGGGTGCTGAGGAGGAGGTGCAG-3'	5'-TCACTGGTGCCCTGCCCCAGG-3'
FLAG-mCHAPb	5'-CACCATGGACTACAAGGATGACGACGACAAGGAGACCACCATCCAAGAGCCC-3'	5'-TCACTGGTGCCCTGCCCCAGG-3'
mCHAPa AA1-298	5'-CACCATGGGTGCTGAGGAGGAGGTG-3'	5'-AAACATAAGCACCCCCTTGGA-3'
mCHAPa AA1-441	5'-CACCATGGGTGCTGAGGAGGAGGTG-3'	5'-CGACAAAGGGCTGAGTGGGAG-3'
mCHAPa AA1-686	5'-CACCATGGGTGCTGAGGAGGAGGTG-3'	5'-GAAGTTACAGGCTTCAGCCCC-3'
mCHAPa AA297-441	5'-CACCATGTTTAAGAAGCGGCGGCAG-3'	5'-CGACAAAGGGCTGAGTGGGAG-3'
mCHAPa AA297-686	5'-CACCATGTTTAAGAAGCGGCGGCAG-3'	5'-GAAGTTACAGGCTTCAGCCCC-3'
mCHAPa AA297-978	5'-CACCATGTTTAAGAAGCGGCGGCAG-3'	5'-CTGGTGCCCTGCCCCAGGCCT-3'
mCHAPa AA442-686	5'-CACCATGGTCCCTGCAGTCAGCCCTACCC-3'	5'-GAAGTTACAGGCTTCAGCCCC-3'
mCHAPa AA442-978	5'-CACCATGGTCCCTGCAGTCAGCCCTACCC-3'	5'-CTGGTGCCCTGCCCCAGGCCT-3'
mCHAPa AA687-978	5'-CACCATGCAGCCACTAGGGGGCAGG-3'	5'-CTGGTGCCCTGCCCCAGGCCT-3'
mCHAPb AA1-69	5'-CACCATGGAGACCACCATCCAAGAGCCCCTC-3'	5'-AAACATAAGCACCCCCTTGGA-3'
mCHAPb AA1-212	5'-CACCATGGAGACCACCATCCAAGAGCCCCTC-3'	5'-CGACAAAGGGCTGAGTGGGAG-3'
mCHAPb AA1-457	5'-CACCATGGAGACCACCATCCAAGAGCCCCTC-3'	5'-GAAGTTACAGGCTTCAGCCCC-3'
z*chap-1*	5'-CACCATGGTAGCAGAGGAGGTGGTG-3'	5'-TCAGTAATGTATGGAGCCAGG-3'
z*chap-2*	5'-CACCATGGTGGCCGAGGAGGTTA-3'	5'-TCAGTGAGGTAAGGTACCAGG-3'

Table S2 *In situ* probe template primers

Gene	Forward primer	Reverse primer	Product size
ChapA/B	5’-ACCATTGCATCCCTGCTAAC-3’	5’-CGCCCAGAGACCTCACTTAG-3’	323
ChapA (124-474)	5’-GAGGAGGTGCAGGTCACATT-3’	5’-CTGAAGAGCCTGGGAAACAG-3’	351
ChapA (353-707)	5’-CTGTTTCCCAGGCTCTTCAG-3’	5’-CCCACCATAGGGATGAGATG-3’	355
ChapB (-65-85)	5’-GGCTTTAAAGGGCCTTGG-3’	5’-CTGCATAGAACGGGTCTTGG-3’	150
zchap-1 (1834-2341)	5’-TCACTGTATATCCCTGCCAGACCA-3’	5’-GCTCTCGAGAAGAGATCCCATCAG-3'	508
zchap-2 (1405-2534)	5’-CACCCAGACCCACTAACAAAGC -3’	5’- GCCTGAGGGATCTGTGACATTTCT -3’	1130